Spring 2010

Comparing the chelating abilities of N-acetylcysteine and N-acetylcysteine amide in vitro for lead poisoning treatment

Weiqing Chen

Department:

COMPARING THE CHELATING ABILITIES OF *N* – ACETYLCYSTEINE AND *N* – ACETYLCYSTEINE AMIDE *IN VITRO* FOR LEAD POISONING TREATMENT

by

WEIQING CHEN

A THESIS

Presented to the Faculty of the Graduate School of the

MISSOURI UNIVERSITY OF SCIENCE AND TECHNOLOGY

In Partial Fulfillment of the Requirements for the Degree

MASTER OF SCIENCE IN CHEMISTRY

2010

Approved by

Nuran Ercal, Advisor
Charles C. Chusuei
Yue-wern Huang

ABSTRACT

Lead poisoning is a perennial and serious health problem around the world. The daily widespread use of lead has dramatically increased the degree and longevity of its exposure to humans, exacerbating the task of lead poisoning treatment. Lead exerts adverse effects on cardiovascular, central nervous, renal, gastrointestinal, and reproductive systems.

The common treatment for lead poisoning is chelation therapy. Chelators were proposed to treat lead poisoning a very long time ago. However, chelators have severe side effects that could cause more problems, in addition to lead poisoning. Therefore, another group of drugs has been suggested --- antioxidants. This type of chemicals not only possesses the chelating abilities for lead cation, but also has only small side effects on tissues. In addition, antioxidants are able to reduce the oxidative stress induced by lead so that a normal antioxidant defense system can be maintained in the human body. Vitamin C, Vitamin E, α-lipoic acid, β-carotene, and *N*-acetylcysteine are the common antioxidants used for treating lead poisoning. In recent years, a new chemical, *N*-acetylcysteine amide, the amide form of NAC, has been synthesized and tested as a promising new drug to treat oxidative stress related disorders.

This research has focused on comparing the chelating abilities that *N*-acetylcysteine (NAC) and *N*-acetylcysteine amide (NACA) have for lead divalent cation. The complex forms of Pb-NAC and Pb-NACA were determined, followed by estimating the amount of lead chelated by these antioxidants. The results showed that there were multiple complex forms for both Pb-NAC and Pb-NACA, and that NACA has a higher affinity for lead than NAC.

ACKNOWLEDGMENTS

I would like to sincerely thank my advisor, Dr. Nuran Ercal, for her support and patience during my graduate study in the Department of Chemistry at Missouri University of Science and Technology.

I also wish to express my sincere gratitude to Dr. Charles C. Chusuei, one of my committee members, for his great guidance in my research work, and much support in the using the facilities. I would like to thank Dr. Yue-wern Huang, my other committee member, from the Department of Biological Sciences, for spending time in reviewing my thesis and giving advice.

I am very grateful to Dr. Nathan Leigh of the Department of Chemistry at University of Missouri – Columbia, for allowing me to use his electrospray ionization mass spectroscopy facility, as well as his helpful discussion.

Funding provided by the National Institutes of Health Academic Research Enhancement Award Grant (2R15ES012167-02A1) and University of Missouri Research Board (RBJ61) are very much appreciated.

I also would like to thank my group members, Dr. Atrayee Banerjee, Dr. Xingsheng Zhang, Mr. Kalyan Manda, and Mr. Joshua Warren Carey. They helped me a lot by discussing the results of my research and operation of the instruments.

Special appreciation goes to my family, my father and mother, and my beloved husband who have always provided support and encouragement in achieving my educational goals.

TABLE OF CONTENTS

LIST OF ILLUSTRATIONS

LIST OF TABLES

1. INTRODUCTION

Lead poisoning is a serious health problem world-wide. Lead and lead chemicals have been commonly used for multiple purposes in different areas over thousands of years. Lead exposure emanates from sources such as paints (Mathee et al., 2007; Gould, 2009), drinking water (Patrick, 2006), food, gasoline (Patrick, 2006), occupational hazards (Shobha et al., 2009), and etc. The widespread use of lead has resulted in lead poisoning becoming a very important toxicity issue. According to a statement issued by the Centers for Disease Control (CDC) in 1985, blood lead levels above 10 μg/dl would be a concern for human health. Children may develop problems in IQ, hearing, and overall developmental growth whereas adults could develop hypertension (Gurer et al., 2000). With elevated blood lead levels ranging from 20 μg/dl to 50 μg / dl, an individual is likely to suffer from abnormal metabolism and cessation of the heme synthesis (Fonte et al., 2007). With much higher blood lead levels (above 50 μg / dl), neuropathy (Catton et al., 1970), encephalopathy (Karri et al., 2008), and even death would result (Figure 1.1).

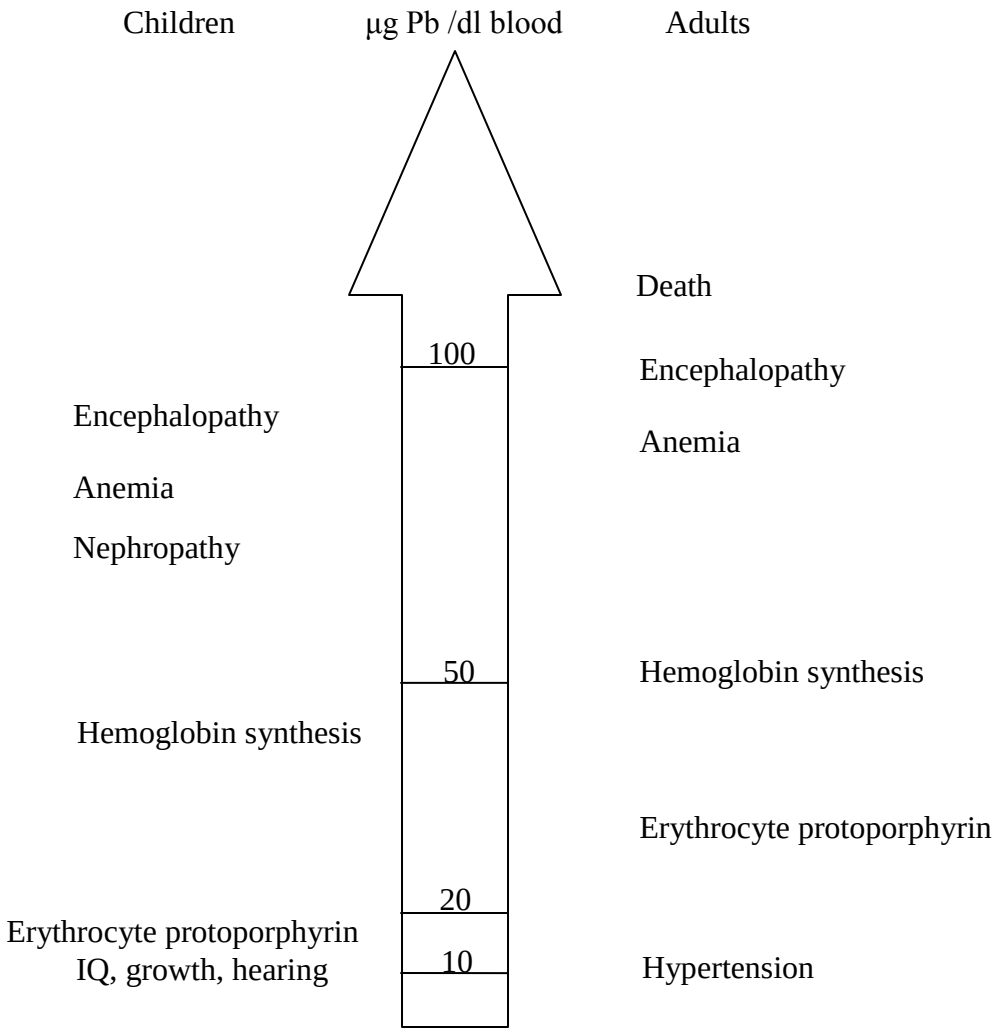

Figure 1.1. The adverse effects of lead poisoning on human health.

2. BACKGROUND

2.1. MECHANISM

Lead poisoning continues to be a health threatening problem. Lead substances can affect human health by inhalation (Landrigan and Todd, 1994), ingestion (Handley et al., 2007) and dermal contact. Lead is toxic to various organs and tissues, and will induce failure of certain enzyme functions and physiological processes in the body, such as the inhibition of heme synthesis (Zhao et al,. 2007), protein oxidation (Sandhir et al., 1994), and lipid peroxidation (Ribarow et al., 1981). A complete understanding of mechanisms governing these processes has not been achieved. However, there are several theories explaining the toxicity of lead.

One mechanism proposed is that lead is able to oxidize glutathione (GSH) (Kidd, 1997), resulting in an imbalance of the antioxidant defense system, and thereby inducing the generation of free radicals. Lead divalent cation has a strong binding capacity for sulfhydryl group-containing proteins and enzymes, and therefore would react with a thiol group containing proteins or enzymes to produce free radicals which would decrease GSH levels (Patrick, 2006), resulting in a decline in the GSH/GSSG ratio (Figure 2.1.). In this scenario, GSH is no longer a natural antioxidant that functions as scavenging reactive oxygen species (ROS), detoxifying carcinogens, and regulating metabolism and the immune system. Rather, the level of free radicals, such as hydrogen peroxide, hydroxyl radical, and lipid peroxide, will be significantly increased in response to the presence of Pb (II), resulting in oxidative stress (Gurer and Ercal, 2000).

Another adverse effect is the failure of heme synthesis (Flora, 2008). Lead divalent cations are able to react with δ-aminolevulinic acid dehydratase (ALAD)

(Mitchell et al., 1977) and ferrochelatase. ALAD, a cytosolic sulfhydryl enzyme, will stop the conversion of two molecules of δ-aminolevulinic acid into porphobilinogen. Therefore, heme biosynthesis in the cell would be terminated at ALAD. Ferrochelatase, an enzyme in the last step of heme synthesis that occurs in the mitochondria, would have much less activity in the presence of lead ions. As a result, these two important enzymes in the heme synthesis would be greatly affected by lead, not being able to perform their normal functions (Figure 2.1). This abnormal process would, in turn, stimulate δ-aminolevulinic acid synthetase. Thus, there would be an increased accumulation of ALA and a decreased formation of porphobilinogen.

Accumulated ALA would induce ROS generation (Ryter, 2000). First, ALA molecules would be converted into the ALA enol form by tautomerization. Secondly, autoxidation of ALA enol generates an ALA• radical and a superoxide anion radical ($O_2^{\bullet -}$). ALA• would further oxidize into iminoALA and produce more superoxide anion radical, forming hydrogen peroxide (H_2O_2) and oxygen. The iminoALA would then react with H_3O^+, forming 2,4-dioxovaleric acid (DOVA) and ammonium ion. Then, the autoxidation of ALA with oxyhemoglobin [Hb-Fe(II)] would produce met-hemoglobin and H_2O_2. The final step is the generation of hydroxyl radicals (•OH) through the metal catalyzed Haber-Weiss reaction (Equations 1-6).

$$\text{ALA (enolic form)} + O_2 \xrightarrow{\text{Fe or Cu}} \text{ALA}^{\cdot} + O_2^{\cdot -} \quad (1)$$

$$\text{ALA}^{\cdot} + O_2 \longrightarrow \text{iminoALA} + O_2^{\cdot -} \quad (2)$$

$$O_2^{\cdot -} + O_2^{\cdot -} + 2H^+ \longrightarrow H_2O_2 + O_2 \quad (3)$$

$$\text{iminoALA} + H_3O_2^+ \longrightarrow \text{DOVA} + NH_4^+ \quad (4)$$

ALA

$$\text{ALA} + O_2 + \text{Fe(II)-Hb} + 2H^+ \longrightarrow \text{ALA}^{\cdot} + H_2O_2 + \text{Fe(III)-Hb} \quad (5)$$

$$H_2O_2 + O_2^{\cdot -} \xrightarrow{\text{Fe or Cu}} O_2 + {}^{\cdot}OH + OH^- \quad (6)$$

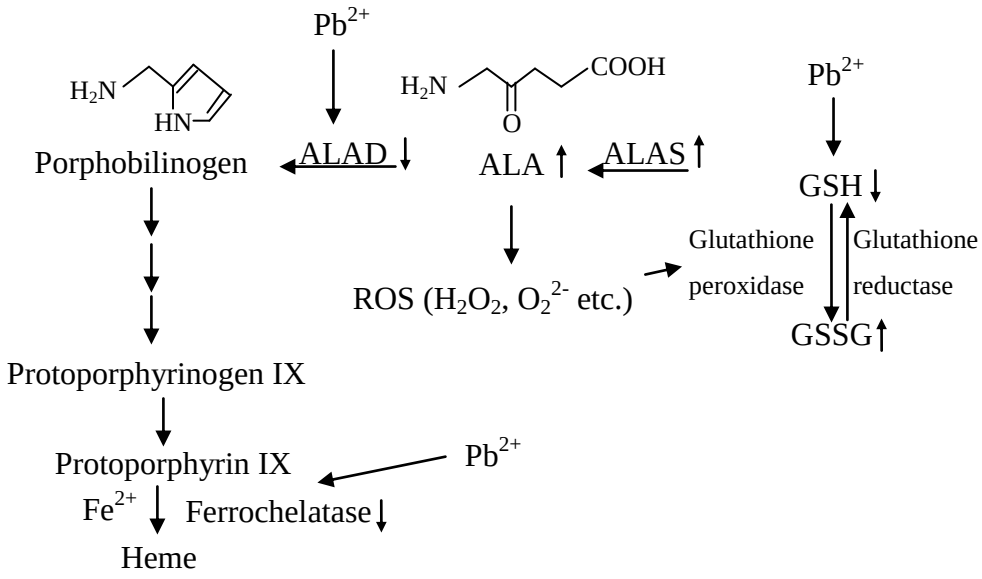

Figure 2.1. The effects of lead on heme synthesis and glutathione metabolism.

2.2. TREATMENT

The major treatment for lead poisoning is chelation therapy (Porru and Alessio, 1996), aimed to remove accumulated lead in the body. The first chelators, used in treating lead poisoning (Kety and Letonoff, 1941) were very effective in removing lead. Ethylenediamine tetraacetic acid (EDTA), a famous and common drug in lead poisoning treatment (Horowitz and Mirkin, 2001; Blanusa et al., 2005; Tzu et al., 2007), is capable of decreasing lead levels in tissue. In the 1950s, $CaNa_2EDTA$, a derivative of EDTA, was first introduced for chelating Pb in acute lead poisoning (Flora et al., 1995). Later, British Anti Lewisite (BAL), and Meso-2, 3-dimercaptosuccinic acid (DMSA) (Xiaojun Fang and Quintus Fernando, 1993; Jie Zhang et al., 2004; Stangle et al., 2007) were also developed for use in chelating therapies for lead poisoning.

However, these chelators have different adverse effects which are extremely harmful. For instance, $CaNa_2EDTA$ itself is toxic for the renal system (Purser et al., 1983), because it will induce cell necrosis. In addition, $CaNa_2EDTA$ is not able to travel through cell membrane and, thus, cannot be used to eliminate lead in the cell. In addition, chelators, such as $CaNa_2EDTA$, are not capable of decreasing reactive oxygen species (ROS) induced by lead, so the oxidative stress still exists in tissues even after chelation therapy is applied. As a result, it is necessary to find other kinds of drugs to treat lead poisoning. Antioxidants, such as Vitamin E and C, selenocystine (Sel) (Aykin-Burns et al., 2006), *N*-acetylcysteine (NAC), *N*-acetylcysteine amide (NACA) (Aykin-Burns et al., 2005; Penugonda et al., 2006), the amide form of NAC, and etc. were considered as promising drugs to treat lead toxicity, because antioxidants not only decrease the blood lead levels, but also help rebalance antioxidant defense systems.

The ideal antioxidant for treating lead poisoning should be: 1) nontoxic; 2) able to easily cross the cell membrane (in which case lead in the cell could be removed by antioxidants as well as in extracellular fluids); and 3) have a strong affinity to the lead divalent cation.

In previous studies, the abilities of decreasing the lead concentration *in vivo* differed widely among various kinds of chelators and antioxidants. This study is aimed to test and compare the chelating ability of two antioxidants --- NAC and NACA, *in vitro*. The two molecules both have a thiol group, which makes possible the binding of Pb(II). NAC has a carboxylic group with a negative charge, while NACA has an amide group on the same site (Figure 2.2). The difference of this one functional group in the molecule may contribute to their different affinities for Pb(II).

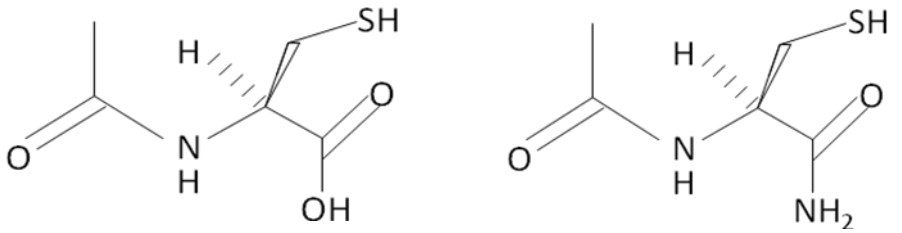

N-acetylcysteine *N*-acetylcysteine amide

Figure 2.2. Molecular structures of *N*-acetylcysteine and *N*-acetylcysteine amide.

The stoichiometry of a Pb-antioxidant complex can be delineated using a UV/vis spectrophotometer. Electrospray ionization mass spectrometry (ESI-MS) was adopted to reveal the structure information of Pb-antioxidant complexes. The amount of lead that

was complexed can be detected by using high performance liquid chromatography (HPLC) and X-ray electron spectroscopy (XPS).

2.3. INSTRUMENTATION

2.3.1. Electrospray Ionization Mass Spectrometry (ESI-MS). Electrospray ionization mass spectrometry is a useful analytical technique. By ionization, analytes of interest can be detected by a mass spectrometer. ESI-MS is very useful to detect macromolecules (Claudia Bich and Renato Zenobi, 2009) without any fragmentation.

2.3.1.1. Theory. Analytes will be first ionized after injection by a high voltage needle, and have certain charges on them without fragmentation. Therefore, the mass – to - charge (m/z) ratio of a molecule in the samples will be unique to others. With its particular m/z ratio, an analyte could be detected by a mass spectrometer.

2.3.1.2. Procedure. Sample solutions will first be atomized using a high voltage needle, during which the analytes become ions with certain charges, because there is a strong electrical field during introduction. Then these ions will enter through a drying gas phase and two pumping stages, at which the ions are separated in the mass analyzer by different m/z ratios. With a mass spectrometer, the analytes could be detected individually by their mass to charge ratio (Figure 2.3).

2.3.1.3. Electrospray and ionization. Analytes in samples will be introduced into to the instrument by a capillary needle, which is applied with a very high voltage, usually from 2 – 5 kV. Then there is a gradient electric – field for the generation of analytes ionization before the drying gas phase. The voltage on the capillary needle could be either positive or negative. However, the mechanism of the ionization process is not

totally understood. It has been suggested that the production of ionic form analytes occurs through two possible models: the ion evaporation model (IEM) and the charged residue model (CRM). In the ion evaporation model, ions are released when the Coulombic repulsion is large enough to overcome the liquid's surface tension (Iribarne and Thomson, 1976). In the charged residue model, solution droplets will have charges when voltage is applied. When the Coulombic repulsion is equal to the surface tension of these droplets, the excess of positive or negative charge in the droplets would be separated from the solution, resulting in single ions (Taflin et al., 1989; Kebarle and Peschke, 1999) (Figure 2.4).

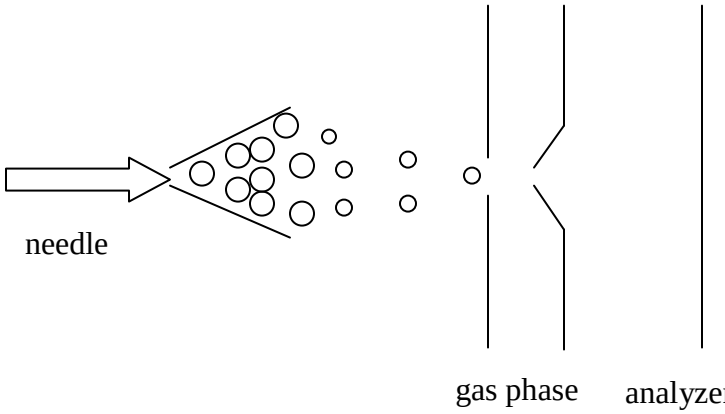

Figure 2.3. Schematic of electrospray ionization spectroscopy.

By ionization, analytes of interest are added or removed by one proton, forming positively charged analytes (like $[M + H]^+$) or negatively charged analytes (like $[M - H]^-$).

In the case of large molecules, there are typically many charge states which are easily detected.

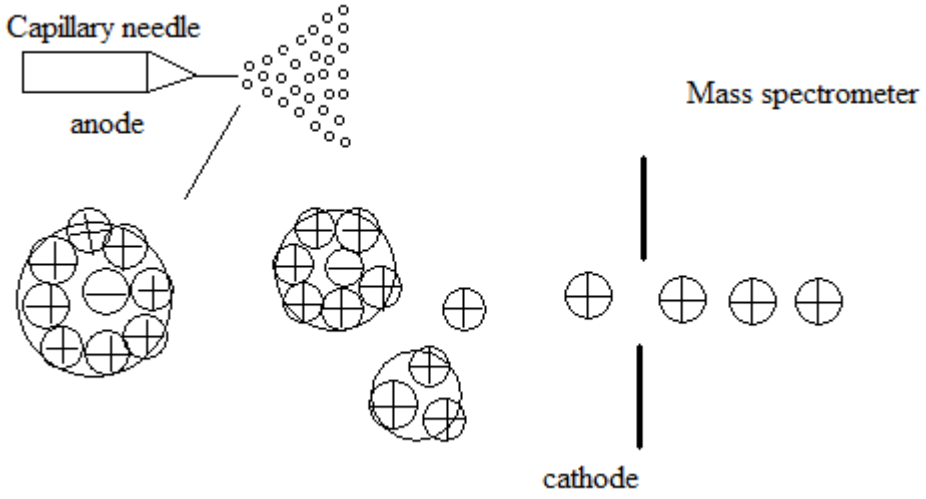

Figure 2.4. An ionization mechanism: the charged residue model.

2.3.2. X-ray Photoelectron Spectroscopy. X-ray photoelectron spectroscopy (XPS) is a surface analytical technique that non – destructively quantifies the elemental composition at the surface of a material at the topmost 50 – 100 Å and to provides chemical oxidation state information of the element examined (Hollander and Jolly, 1970).

2.3.2.1. Theory. When soft X-rays impinge onto the surface of a material being analyzed, the electrons in various valence orbitals will be ejected via a photoelectric effect. The kinetic energy of these emitted electrons are measured and recorded, providing chemical information.

X-ray photoelectron spectroscopy provides qualitative and quantitative

information about the surface of a material. Every elemental transition has its own characteristic kinetic energy, which appear in the binding energy spectra recorded by XPS. The binding energy range typically spans between 0 and 1250 eV. If a material contains carbon, and oxygen elements, there will be signal peaks at around 285 eV (Barr, 1994), and 535 eV (Vaneica Y. Young and Kathryn R. Williams, 1999), respectively. The percentage of each element can be quantified by examining their normalized integrated peak areas.

Small shifts in the binding energy indicate a different oxidation state of this particular element. Assuming that there are no final state effects, the chemical shift is arises from the coordination between this element and other elements in the same material. In Figure 2.5 (Siegbahn et al., 1967), the changes in the signal peak position are indicated in the binding energy spectra due to changes in the oxidation state at C1s orbital (Barr, 1994). In an electron deficient - environment, the binding energy increases; in an electron – rich environment the binding energy decreases (Hagstrom et al., 1964).

2.3.2.2 Mechanism The emission of photoelectrons is initiated by the irradiation of an X-ray with a certain known energy, *hv* (Figure 2.6). Assuming the 1s orbital of element A, for example, has one photoelectron displaced by the X-ray beam, the reaction occurring for element A would be:

$$A + h\nu \longrightarrow A^{+*} + e^{-} \qquad (7)$$

In this equation, A is a certain atom, *hv* is the energy of the X-ray beam, A^{+*} is a positively charged ion, and the electron, e^{-}, is the escaping electron from the 1s orbital of atom A.

The kinetic energy could be calculated by X-ray photoelectron spectroscopy using the equation:

$$KE = h\nu - BE - \Phi \quad (8)$$

KE stands for the kinetic energy of the emitted electron, $h\nu$ for the energy of the X-ray beam, BE for the binding energy of the electron from a particular orbital being detected, and Φ for the work function of the spectrometer. The work function and the X-ray energies remain constant when using the same instrument for measurement. Therefore, the binding energy of this element could be determined by:

$$BE = h\nu - KE - \Phi \quad (9)$$

2.3.2.3 Instrumentation A typical X-ray photoelectron spectroscopy system consists of an X-ray source, a sample holder, an analyzer, a detector and a place for detection within an ultra – high vacuum system (UHV) (Figure 2.7).

In the set – up used to acquire the data in this thesis, monochromatic soft X-rays were produced by a Mg Kα anode (hν = 1253.6 eV). A sample holder was maintained at a proper position in the ultra – high vacuum (UHV) for a suitable detection of electrons by the spectrometer. UHV conditions were required to insure the flight of photoelectrons into the detector analyzer and to reduce contamination on the material surface. The pressure of this vacuum system was maintained between 10^{-8} Torr to 10^{-10} Torr before, during and after analysis. The analyzer used for these experiments was a double-pass cylindrical mirror analyzer with two spherical grids. Electrons were retarded using these two grids to focus the photoelectrons into the detector. Usually two cylindrical mirror analyzer are used together to increase the resolution in XPS systems.

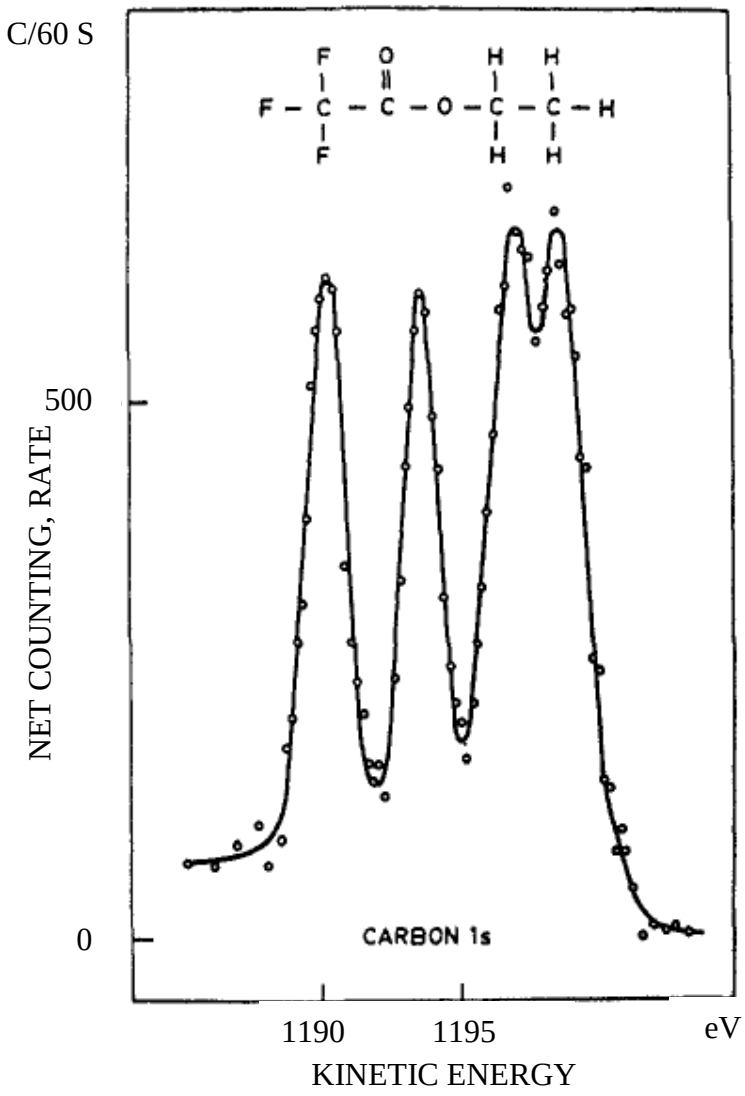

Figure 2.5. Carbon 1s X-ray photoelectron spectrum for ethyl trifluoroacetate.

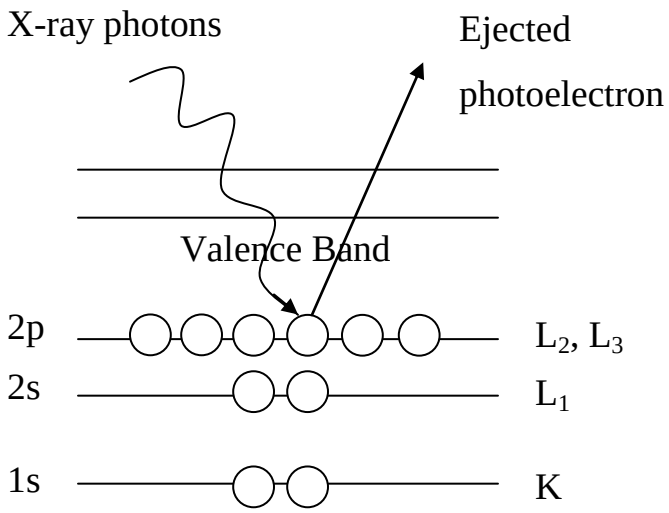

Figure 2.6. Mechanism of X-ray photoelectron spectroscopy.

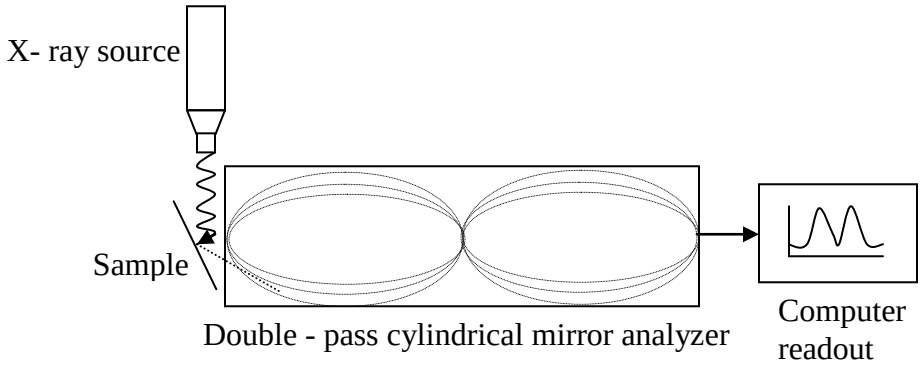

Figure 2.7. Schematic of X-ray photoelectron spectroscopy.

3. MATERIALS AND METHODS

3.1. CHEMICALS

N-acetylcysteine amide was provided by Dr. Glenn Goldstein (David Pharmaceuticals, New York, NY, USA). High-performance liquid chromatography (HPLC) grade solvents and Na_4EDTA were purchased from Fisher Scientific (Fair Lawn, NJ). All other chemicals including *N*-acetylcysteine, were purchased from Sigma - Aldrich (St. Louis, MO).

3.2. DETERMINAITON OF THE STOICHIOMETRY OF Pb - ANTIOXIDANT COMPLEX

A stock solution of lead acetate and antioxidants of the same concentration were prepared and maintained at a temperature between 0°C and 10°C. The volume ratio of Pb(II) and antioxidants varied from 7:1 to 1:3 according to Job's method (MacCarthy et al., 1976). Job's method is a quick and simple way to determine the stoichiometry of a complex. When the volume ratio of two molecules is equal to their stoichiometric ratio, the amount of the complex formed reveals a maximum. Figure 3.1 shows an example of which the absorbance reaches to the maximum when the volume of the two reacting molecules are at 1 to 1 ratio, so x, one molecule's volume over the total volume, is equal to 0.5. The stoichiometry is 1: 1. Each sample was tested under UV light, between wavelengths of 300nm and 190nm which were then recorded.

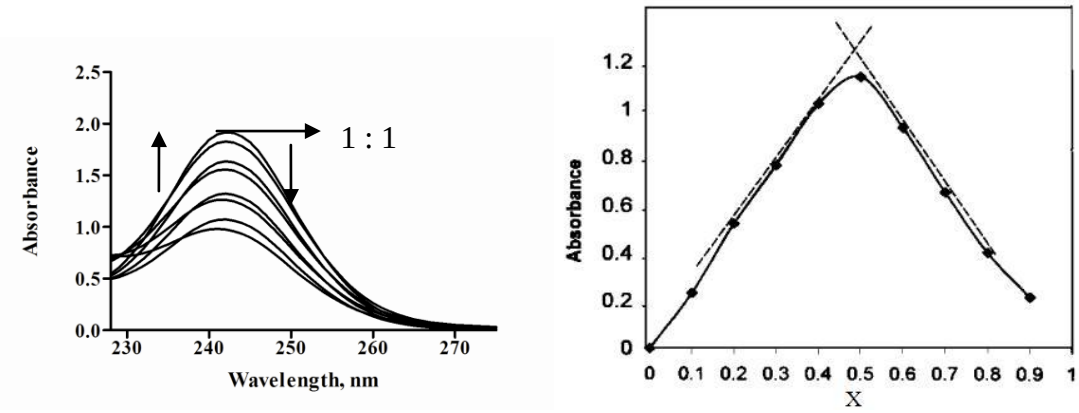

Figure 3.1. Determination of stoichiometry using Job's method.

3.3. STRUCTURE INFORMATION OBTAINED FROM ESI-MS

Lead acetate was dissolved with Na_4EDTA, NAC, and NACA in doubly distilled deionized water with a 1:1 ratio, respectively. The solutions containing Pb-antioxidant complex were then analyzed by using a Thermo-Finnigan TSQ7000 triple-quadrupole mass spectrometer. The heated inlet capillary was kept at 250°C and the electrospray needle voltage was maintained at 4.5 kV. All voltages were chosen to maximize ion transmission and minimize unwanted fragmentation.

3.4. DETECTION OF COORDINATED LEAD – THIOL GROUPS IN THE ANTIOXIDANTS BY HPLC

Sample solutions were prepared with Pb acetate and antioxidants at ratios of 0:1, 0.5:1, 1:1, 2:1 and 4:1. These solutions were introduced into high performance liquid chromatography (HPLC). The HPLC system from Thermo Electron Corporation is composed by a Finnigan Surveyor autosampler Plus, a Finnigan Surveyor LC pump Plus,

and a Finnigan Surveyor fluorescence Plus detector (λ_{ex}=330 nm, and λ_{ex}=376 nm). The HPLC column was a Reliasil C_{18} column (5 μm packing material) with 250×4.6 mm i.d. (Orochem technologies INC. Lombard, IL, USA).

An isocratic program was used for Cysteamine hydrochloride testing. In this program, mobile phase A was composed of a volume ratio of 70:30 acetonitrile and HPLC- grade water, with 0.1% acetic acid and 0.1% o-phosphoric acid. The flow rate of this program was 1.000 ml/min, the percentage of mobile phase A was 100%, and the running time was 20 mins.

A gradient separation method was used for the detection of NAC and NACA (Wu et al., 2006). Mobile phase A was composed of a volume ratio of 70:30 acetonitrile-HPLC-H_2O (v:v) with 0.05% acetic acid, and mobile phase B was composed of a volume ratio of 70:30 acetonitrile-HPLC-H_2O (v:v) with 0.04% o-phosphoric acid.

The running time for mobile phase A was from 0.1 min to 6.00 min, the flow rate was 0.7 ml/min, and the volume was 100%. The running time for mobile phase B was from 6.10 min to 10.00 min (Figure 3.2), the flow rate was 1.7 ml/min, and the volume was 100% (Wu et al., 2006).

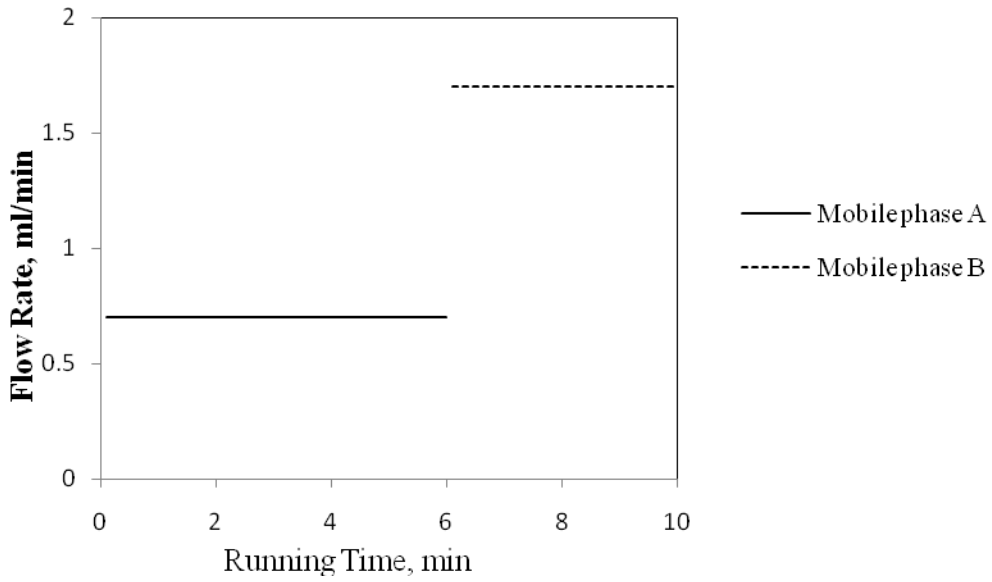

Figure 3.2. A gradient method for NAC and NACA's HPLC detection.

Stock solutions of the studied antioxidants were prepared by dissolving 6.5 mg NAC (NACA: 6.5mg) in doubly distilled deionized water, making a concentration of 1mM. This 1mM concentration of NAC was then diluted to produce 100μM, 10μM, 1μM and 0.1μM concentrations. Stock solutions of lead acetate were prepared by dissolving 15.2 mg Pb acetate trihydrate in doubly distilled, deionized water, making a 1 mM Pb(II) solution. The 1 mM lead acetate was then diluted into 100 μM and 10 μM.

A calibration experiment was performed first to elucidate the relationship of the peak area and the concentration, in which the concentrations varied: 2.5 nM, 12.5 nM, 25 nM, 50 nM and 125 nM. Table 1 details about the preparation of the standard solutions.

Table 1. Calibration solution preparation for HPLC detection

Conc. (nM)	Stock solution (μl)	H_2O (μl)	NPM (μl)	HCL (μl)
0	0	250	750	10
2.5	25.0 (0.1μM)	225.0	750	10
12.5	12.5 (1μM)	237.5	750	10
25	25.0 (1μM)	225.0	750	10
50	50.0 (1μM)	200.0	750	10
125	12.5 (10μM)	237.5	750	10

The experiment was divided into two parts, 0 hour and 1 hour time courses. For the 0 hour experiment, sample solutions were quickly prepared from the stock solution within 5 min; and then directly introduced to the autosampler system of the HPLC. Table 2 shows the components of sample solutions. In the case of the 1 hour experiment, a stock solution was incubated in a 37 °C water bath for 1 hour, and then used to prepare the remaining sample solutions. In all of the sample stock solutions, the concentration of NAC was 1 μM, and the concentration of lead acetate varied: 0, 0.5 μM, 1 μM, 2 μM and 4 μM. These sample solutions were finally made into a 12.5 nM concentration solution.

Table 2. Sample solution for HPLC detection

Ratio of NAC : Pb	Stock solution of NAC (ml)	Stock solution of Pb acetate (ml)	H_2O (ml)
1 : 0	5.00 (1 μM)	0	0
1 : 0.5	0.50(10 μM)	0.25 (10 μM)	4.25
1 : 1	0.50 (10 μM)	0.50 (10 μM)	4.00
1 : 2	0.50 (10 μM)	1.00 (10 μM)	3.50
1 : 4	0.50 (10 μM)	2.00 (10 μM)	2.50

3.5. DETECTION OF THE PERCENTAGE OF LEAD BEING CHELATED BY USING XPS

X-ray photoelectron spectroscopy (XPS) was performed in an ion-pumped Perkin-Elmer PHI 560 system using a PHI 25-270AR double-pass cylindrical mirror analyzer. A magnesium Kα anode was operated at 15 kV and 250W with photon energy of 1253.6 eV. The system pressure did not exceed $1x10^{-8}$ Torr during scans. The pass energy used for high resolution XPS was 50 eV (0.1 eV/step and 90 ms/step). A 99.99% purity Ta foil (Cross Co., Moonachie, NJ) was used as a metal support for the Pb-antioxidant film. A 0.1 ml aliquot of Pb acetate-antioxidant, with a ratio of 5:1 solution (lead acetate 2.5 mM : antioxidant 0.5 mM) solution was loaded onto the 1cm x 1cm x 0.1 mm square surface, and then introduced into a turbopumped antechamber to evaporate the liquid and outgas the sample prior to introduction into the UHV for XPS analysis. The Ta substrate (spot-welded to electrical leads from the sample probe) was cleaned by resistive heating by passing 12 amps through the Ta foil using a power supply (Hewlard – Packard 6259B DC power supply). The surface was heated to 1200 K, which sufficiently removed all of the Pb-antioxidant adsorbates. The C 1s level at 284.7 eV was used for charge correction (Barr, 1994).

3.6. POINT OF ZERO CHARGE VALUE DETERMINATION OF NAC AND NACA

Solutions with pH values from 1 to 12 were prepared with HCl and NaOH solutions with 0.3 ml aliquots of each pH solution added into 5 ml glass tubes containing 150 mg of NAC and NACA powder, respectively. The pH of each of the 12 tubes was measured by a pH meter. After a16 hour incubation in a refrigerator, the final pH values

of each tube was measured again and plotted to determine the point of zero charge values (Park and Regalbuto, 1995).

4. RESULTS

4.1. SEVERAL COMPLEX FORMS

Structure information of a Pb-antioxidant complexes were obtained using UV - vis spectrophotometry and ESI – mass spectroscopy. Job's method was applied to determine the stoichiometry of the Pb-antioxidant complex using a UV - vis spectrophotometer. Figure 4.1.A shows the spectra for signals of a Pb-Na_4EDTA complex, indicating that 246 nm was the wavelength of maximum absorbance. According to Job's method, x was 0.5, indicating that the stoichiometry of this complex was 1:1 ratio. This result is consistent with the literature (Gupta et al., 2007). Figure 4.1.B depicts the result for a Pb-NAC complex, also from Job's method. From the spectra, the highest absorbance of the signal was at 275 nm. The x was 0.286, so the stoichiometric ratio was 2.5:1for Pb:NAC. Figure 4.1.C reveals the spectra of a Pb-NACA complex. There were the same as for the Pb-NAC complex, and 275 nm was the wavelength with the maximum absorbance. The x was 0.4; therefore, the stoichiometric ratio was 1.5:1for Pb-NACA.

The stoichiometries of Pb-NAC and Pb-NACA were very different from each other. The 2.5:1 ratio of Pb-NAC indicated that there was more than one single complex, which was the case with Pb-NACA with its stoichiometry of 1.5:1.

Since there was more than one complex formed in Pb-NAC and Pb-NACA, it was not possible to determine their binding constants by just using UV-vis spectroscopy. Job's method is only effective when only one complex formed in the solution, so an accurate determination of the stoichiometry could not be made.

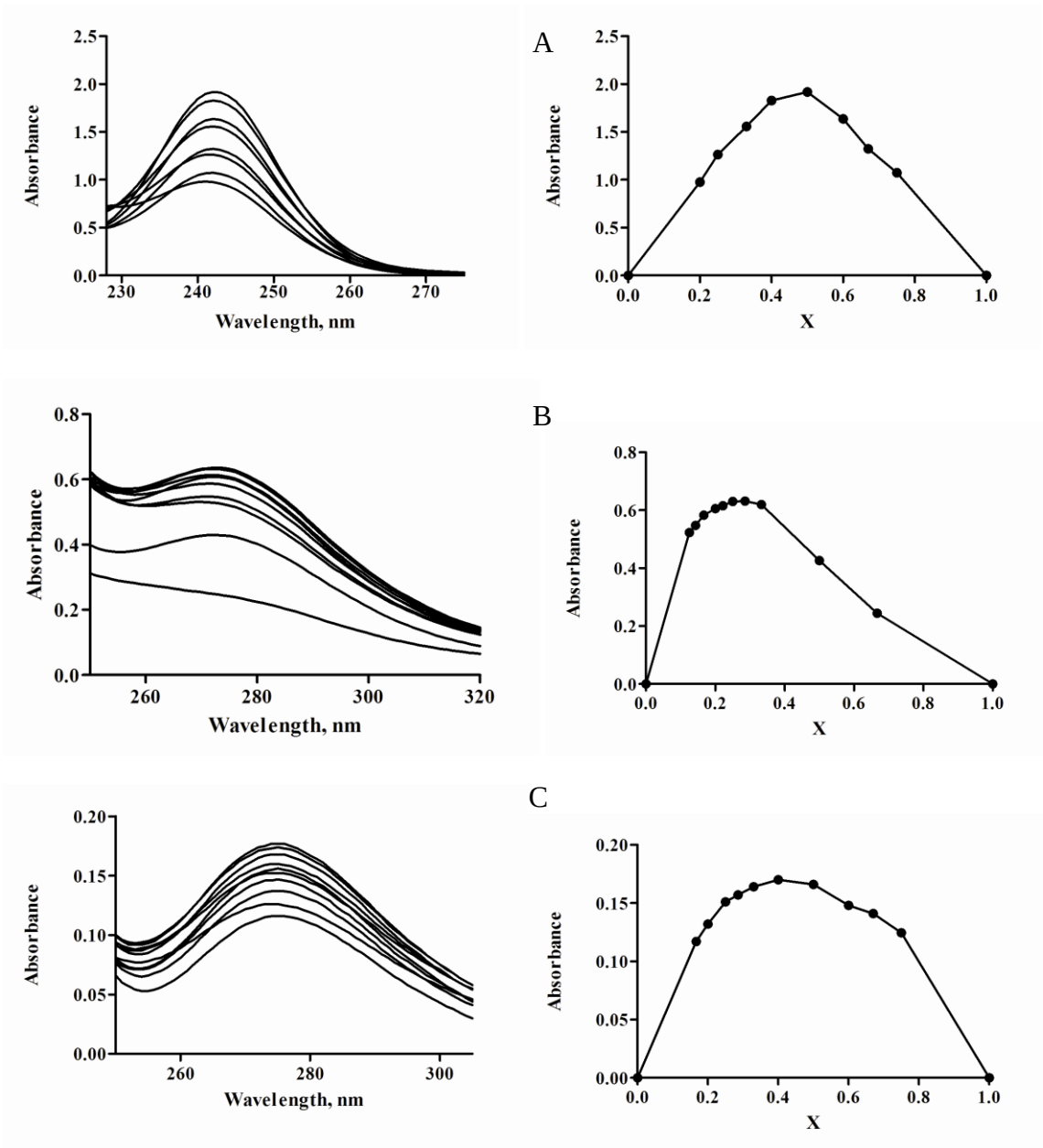

Figure 4.1. Plot of Job's method and spectra for a) Pb-EDTA complex; b) Pb-NAC complex; and c) Pb-NACA complex.

Electrospray ionization, coupled with mass spectrometry (ESI-MS), was applied to detect the major complex in Pb-NAC and Pb-NACA complexes. Figure 4.2 shows the signal of $[Na_3EDTA\text{-}Pb]^+$ at 565.09 m/z, a 1:1 ratio of Pb(II) : EDTA in the complex. This result was consistent with the result obtained in the stoichiometry by using UV-vis spectrophotometry. Figure 4.3 was the spectra of signal for the Pb(II) and NAC solution. Pb(II) was able to coordinate with NAC by ratios of 1:1, 2:1, 2:2, and 3:2, resulting in a signal for $[Pb\text{-}NAC]^+$ at 369.77 m/z, a signal for $[Pb\text{-}NAC\text{-}Pb\text{-}H_2O]^+$ at 591.82 m/z, a signal for $[NAC\text{-}Pb\text{-}NAC\text{-}Pb]^+$ at 736.80 m/z, and a signal for $[Pb\text{-}NAC\text{-}Pb\text{-}NAC\text{-}Pb]^+$ at 942.73 m/s. Their percentages of the total Pb-NAC complexes were 76.5%, 14.5%, 6.5%, and 2.5%, respectively. These complexes all contribute to the multi-form of Pb-NAC. Figure 4.4 reveals the spectra for the Pb acetate and NACA solution, in which case the signal was not the same as for Pb-NAC. There were three major complex signals. One was a signal $[Pb\text{-}NACA\text{-}H]^+$ at 368.93 m/z. Two other peaks were observed at 529.08 m/z and 575.04 m/z for $[Pb\text{-}(NACA\text{-}NACA)\text{-}H]^+$ and $[Pb\text{-}NACA\text{-}Pb]^+$. Their percentages of the composition were 92.2%, 4.8% and 3.0%, as shown in Table 3.

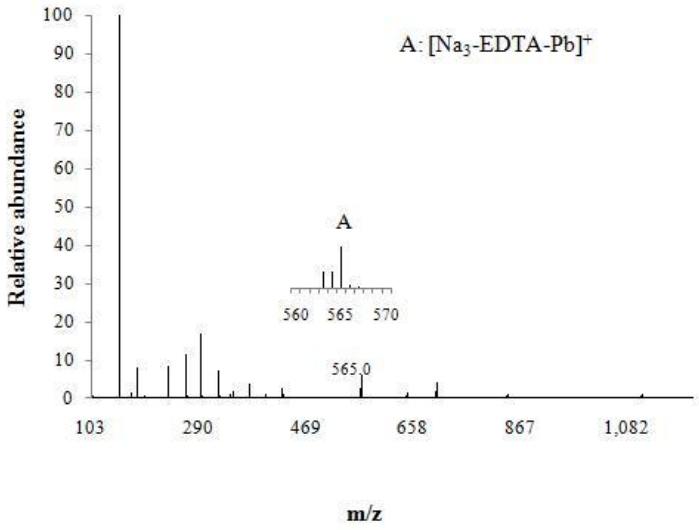

Figure 4.2. Spectra of a derivatized Pb-EDTA from ESI-MS.

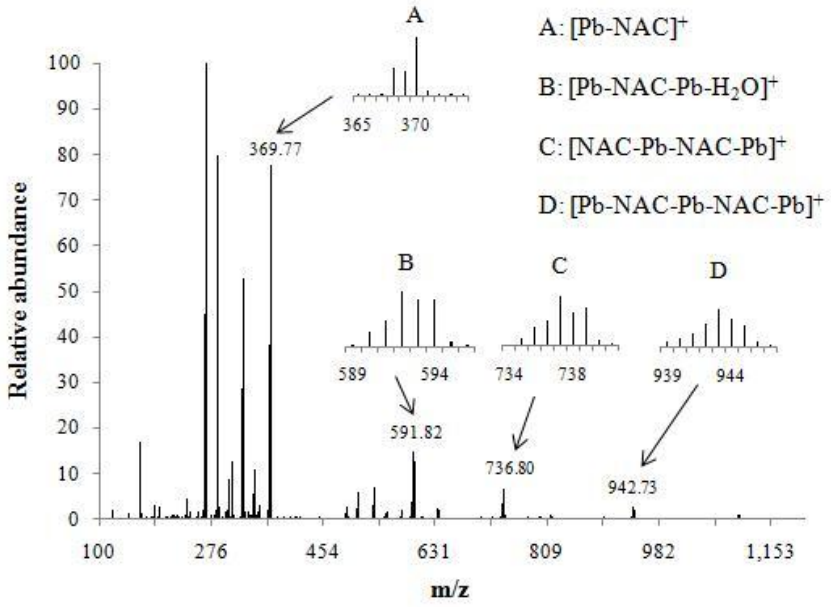

Figure 4.3. Spectra of a derivatized Pb-NAC from ESI-MS.

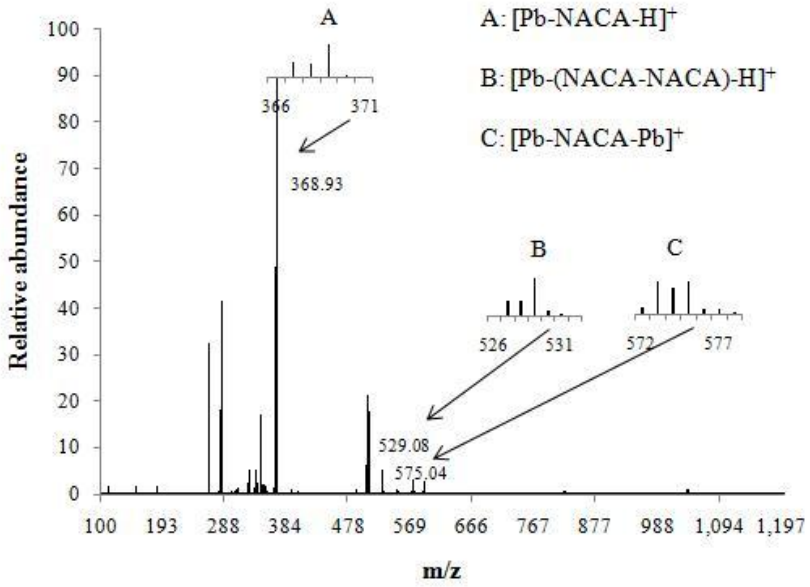

Figure 4.4. Spectra of a derivatized Pb-NACA from ESI-MS.

Table 3. Composition of Pb-antioxidant complexes obtained from ESI-MS

	Mass to charge ratio (m/z)	Substance	% of the total Pb-antioxidant substances
Na_4EDTA	565.09	$[Na_3\text{-EDTA-Pb}]^+$	100%
NAC	369.77	$[\text{Pb-NAC}]^+$	76.5%
	591.82	$[\text{Pb-NAC-Pb-H}_2\text{O}]^+$	14.5%
	736.80	$[\text{NAC-Pb-NAC-Pb}]^+$	6.5%
	942.73	$[\text{Pb-NAC-Pb-NAC-Pb}]^+$	2.5%
NACA	368.93	$[\text{Pb-NACA-H}]^+$	92.2%
	529.08	$[\text{Pb-(NACA-NACA)-H}]^+$	4.8%
	575.04	$[\text{Pb-NACA-Pb}]^+$	3.0%

4.2. CHELATING ABILITIES

Upon examination of the Pb-antioxidant complex forms and their relative abundances, it was possible to estimate the chelating abilities of *N*-acetylcysteine amide and *N*-acetylcysteine to lead divalent cation *in vitro*.

The chelating ability was evaluated by quantifying the percentage that Pb(II) coordinated to the antioxidants. HPLC was applied to determine the amount of antioxidants that had been coordinated. Cysteamine hydrochloride, NAC and NACA are mono-thiol antioxidants that contain a sulfur-hydrogen functional group. By adding N-(1-pyrenyl) maleimide (NPM) to the sample, the thiol group in the compounds coordinated with NPM, formed a highly fluorescent complex for detection. A gradient program was used for NAC and NACA in the HPLC system, so that the thiol group could be both qualified and quantified. In the case of Cysteamine, an isocratic program was applied. The retention times for NAC, NACA and Cysteamine were around 4.8 min, 5.2 min and 17.2 min, respectively. Figure 4.5 shows the declining trend of Cysteamine with the increase of Pb acetate in a mixed solution. At a ratio of 1:1, there was a 19.0% decrease in free Cysteamine concentration without any incubation, and a 33.5% decline after 1 h incubation in a 37°C water-bath. Figure 4.6 also reveals a declining trend for available NAC by using more Pb acetate. At a ratio of 1:1, 10.4% NAC reacted with Pb(II) with no incubation, and 17.8% NAC with 1 h incubation in a 37°C water-bath. The results were the same with NACA (Figure 4.7). With the addition of more Pb(II) acetate, the decrease in free Cysteamine, NAC, and NACA was more obvious (Table 4). In addition, there was a great difference in the amount of reacted antioxidants between no incubation and 1 hr incubation at 37°C temperature. There were more antioxidants being

coordinated with lead acetate after 1 h of incubation, indicating a time period for a reaction between the antioxidants and Pb(II).

Based on the amount of antioxidants that chelate Pb(II) and the percentage of the major complex forms, the percentage of Pb(II) that had been reacted by NAC and NACA could be estimated. In Pb-NAC, the major part is $[Pb\text{-}NAC]^+$ with 76.5%. In this complex, the ratio of Pb (II) to NAC was 1:1. From the results obtained from HPLC, the total NAC reacted was 10.1% at a 1:1 ratio to the group with no incubation. Therefore, the total amount of lead chelated in the complex $[Pb\text{-}NAC]^+$ would be 76.5%×1×10.1%=7.7%. The total amount of Pb (II) being bound by NAC was estimated by adding the percentage of lead reacted with all of the complex forms in the Pb-NAC solution. The amount of Pb(II) complexed would be 11.7%. The percentage of lead chelated by NACA was 21.8%.

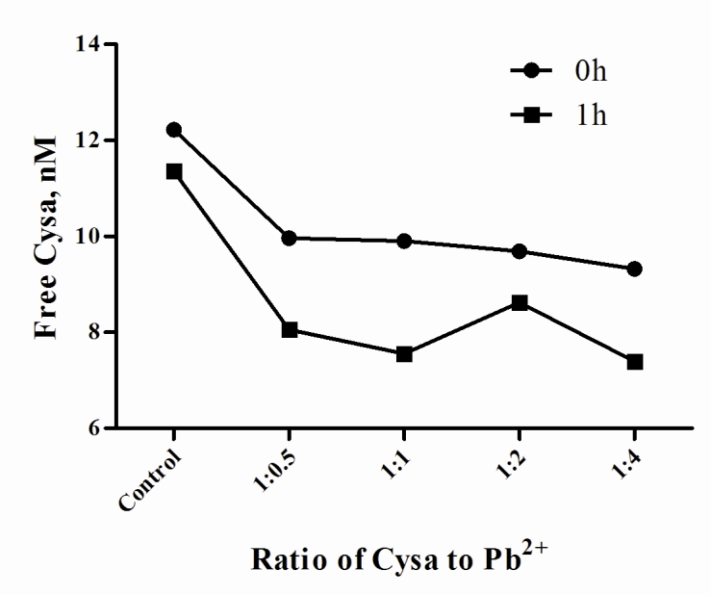

Figure 4.5. Amount of Cysteamine available in the Pb(II) and Cysteamine solution.

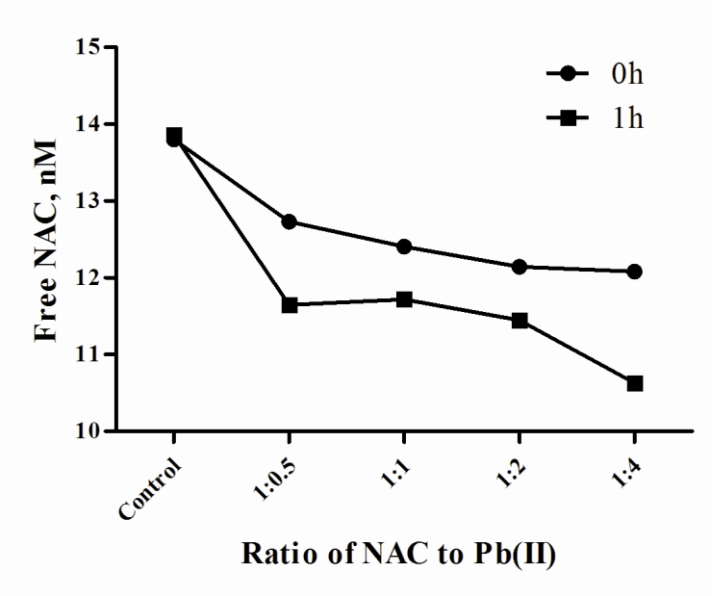

Figure 4.6. Amount of NAC available in the Pb(II) and NAC solution.

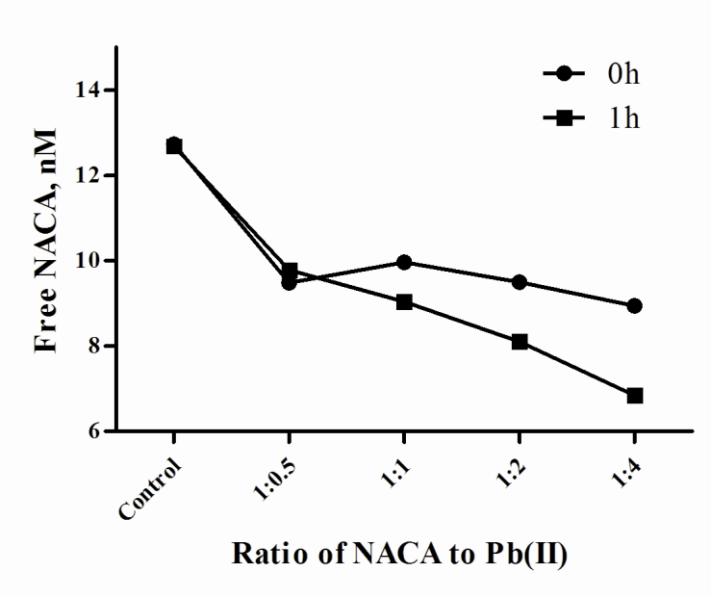

Figure 4.7. Amount of NACA available in the Pb(II) and NACA solution. (The filled bar stands for 0h incubation result, and the blank bar for 1h incubation result at 37°C.)

Table 4. Percentage of antioxidants that have been reacted with Pb(II)

	1:0.5		1:1		1:2		1:4	
	0h	1h	0h	1h	0h	1h	0h	1h
NACA	25.5%	22.9%	21.7%	28.7%	25.4%	36.1%	29.7%	46.1%
NAC	7.8%	16.0%	10.1%	15.5%	12.0%	17.4%	12.5%	23.3%
Cysteamine	18.5%	29.1%	19.0%	33.5%	20.7%	24.1%	23.7%	34.8%

X-ray photoelectron spectroscopy was also applied to evaluate the chelating abilities of antioxidants. The changes of binding energy at a Pb 4f orbital were observed by analyzing the peaks, and comparing them to the control group (Figure 4.8). There were two peaks at the Pb 4f orbital for the control group, due to the spin orbital coupling, which only contained lead acetate; the two peaks were at 138.4eV and 143.3eV. In the case of samples with Pb(II) dissolved with Na_4EDTA, NAC and NACA separately, two additional peaks were around 138.4eV and 143.3eV, apart from the control group (Figure 4.9, a graph for one Pb-NAC sample at a Pb 4f orbital). Therefore, four peaks of Pb 4f were curve-fitted for the sample groups, deconvoluted using the analysis software, CasaXPS VAMAS software version 2.2 (Devon, United Kingdom). The two additional peaks, not observed in the control, signified the oxidation state in which Pb was bound to the antioxidants.

The Pb 4f chemical oxidation states were quantified by measuring their XPS integrated peak areas. The peaks of the control group at 138.4eV and 143.3eV were denoted as components A and B in solid lines, and the two additional peaks that appeared in the samples were components C and D in dot lines. The percentage of the area of

component C, plus that of component D, over the areas of all of the peaks, is equal to the percentage of Pb bound, as shown in the equation

$$\text{Percentage of Pb(II) bound} = \frac{C+D}{A+B+C+D} \quad (10)$$

The sum of the percentage of component C and component D is shown in Table 5, revealing the trend that NACA had a higher affinity with Pb (II), as compared to the Na_4EDTA and NAC groups (Figure 4.10). In all of the sample groups, 5mM Pb acetate reacted with 1mM chelator/antioxidants. In the Na_4EDTA group, 11.6% of Pb was bound, and in the NAC sample, 10.3% of Pb was bound, while in NACA, 21.6% of the lead was absorbed, twice the percentage of the Pb-Na_4EDTA and Pb-NAC complexes.

There was only one functional group difference between NAC and NACA. Since NACA is the amide form of NAC, it was anticipated that the two antioxidants would have similar chelating abilities to Pb(II). However, NACA had a much higher affinity to Pb(II), according to results from the XPS experiment. Thus, a study in determination of the point of zero charge was carried out to understand the underlying reason for this difference.

4.3. POINT OF ZERO CHARGE (PZC)VALUES

Figure 4.11 shows the initial and final pH values for both NAC and NACA. The point of zero charge (PZC) for NAC was at pH=2.0, and for NACA, the pH was 5.1. The pH value of the sample solution, in which Pb(II) dissolves with antioxidants, was at pH 4.6. From the perspective of surface chemistry, if a solid surface with a PZC is higher than that of the surrounding aqueous solution, the surface will become protonated and adopt a positive charge. Conversely, a solid surface with a PZC lower than that of the surrounding solution is prone to be hydroxylated, adopting a negative surface charge.

Clear difference in PZC between NAC and NACA were observed. NACA's point of zero charge value was higher than that of the sample solution, while NAC's was lower than that of the solution. We attribute the greater amenability of Pb(II) absoption to the accumulation of positive charge on the NACA substrate.

Table 5. Percentage of Pb (II) that has been chelated by antioxidants

	Component C %	Component D %	C+D %
EDTA	5.8 ± 1.4%	5.8 ± 2.8%	11.6 ± 2.6%
NAC	5.4 ± 2.3%	5.3 ± 1.3%	11.2 ± 3.5%
NACA	10.5 ± 2.7%	11.2 ± 1.9%	21.6 ± 0.9%

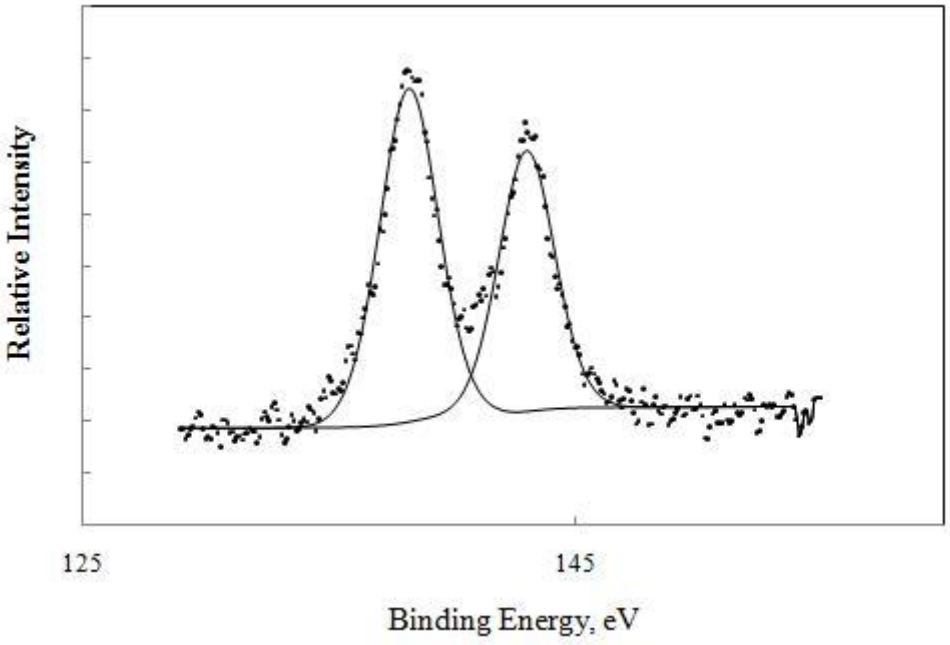

Figure 4.8. Control spectra for Pb 4f orbital.

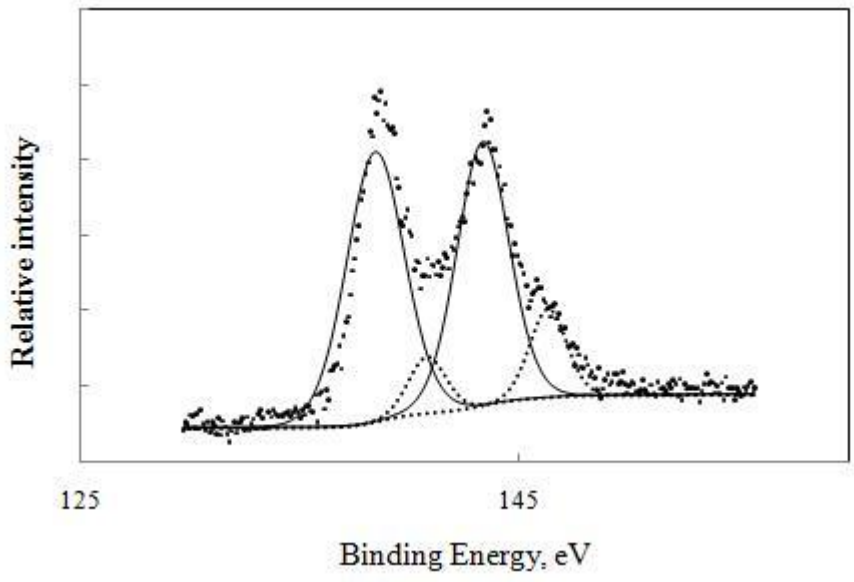

Figure 4.9. A sample spectra for Pb 4f orbital. This sample was composed of ratio 5:1 Pb acetate and NAC in the solution.

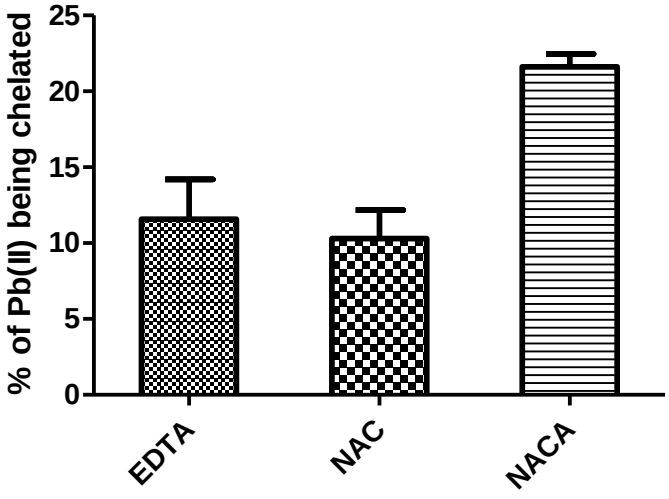

Figure 4.10. Percentage of Pb(II) being chelated by Na_4EDTA, NAC and NACA.

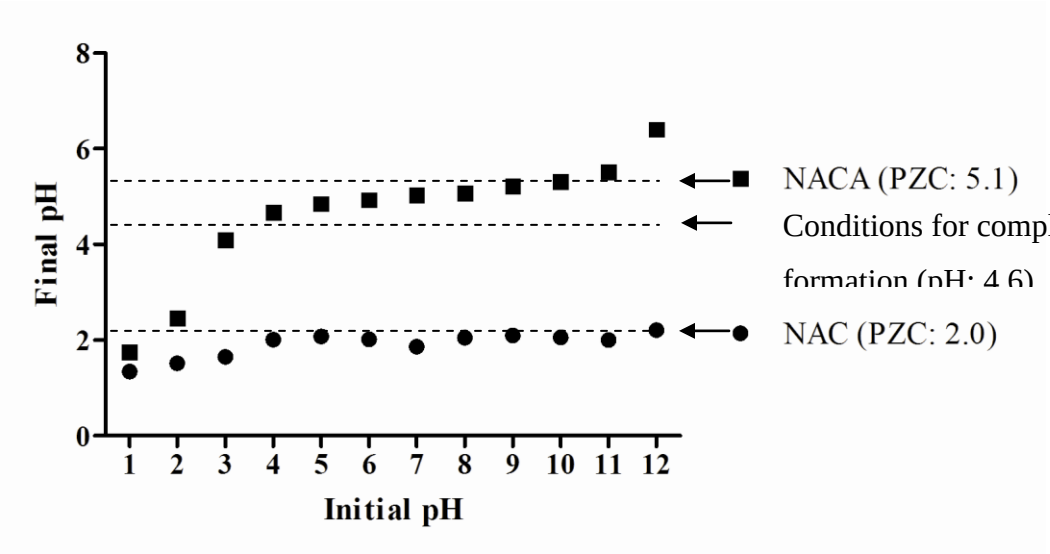

Figure 4.11. Point of zero charge values for NAC and NACA.

5. DISCUSSION

Because of the harmful side effects of chelators, patients with low blood lead levels are encouraged to leave areas prone to lead exposure. Only individuals who have blood lead levels as high as 45 μg / dL or above, will be treated with chelation therapy. The recent application of antioxidants provides a better treatment for lead poisoning, because antioxidants are able to decrease the lead level, as well as relieve the oxidative stress being induced.

N-acetylcysteine is the most popular drug among these antioxidants. This antioxidant can be well absorbed by human bodies, and can cause a further decline in blood lead levels. As a result, its amide form, *N*-acetylcysteine amide, is produced, which might be better for decreasing lead levels. Therefore, it is necessary to compare the chelating abilities of the two similar compounds *in vitro*.

Based on the Job's method, it was possible to determine the stoichiometry of a complex. However, this method was restricted to determining only one complex. The data from UV-vis spectroscopy showed the consistency with literature of the Pb-EDTA 1:1 ratio stoichiometry, while the ratios of the Pb-NAC and Pb-NACA complexes were 2.5:1 and 1.5:1 ratio, respectively. The ratios of Pb-NAC and Pb-NACA indicated that there were several complexes in the samples. As a result, it was not possible to determine the exact stoichiometries for the Pb-NAC and Pb-NACA complexes, or their binding constants, by using UV-vis spectroscopy.

To further understand the coordination between Pb and the antioxidants, the molecular structures of Pb-NAC and Pb-NACA complexes were necessary. One of the ways was to determine the direct coordination between lead and the antioxidants by

making their crystals. Crystallization of the complexes had been unsuccessfully tried. Although conditions of experiment were changed, such as the concentrations of lead acetate and antioxidants in a solution, incubation temperature, time and solvent, there was no crystal formation in the end. Another way to determine coordination was to use ESI mass spectroscopy to detect the mass to charge ratio of a certain signal and to determine whether there is a lead isotope peak. Since this ESI-MS system produces positron, every signal peak stands for a compound with one positive charge. With the known molecular weight of lead acetate, Na_4EDTA, *N*-acetylcysteine and *N*-acetylcysteine amide, the forms of the complexes were calculated and determined. From the results obtained, we found four complex forms in the Pb-NAC sample, with ratios of 1:1, 2:1, 2:2 and 3:2. Among them, the 1:1 ratio complex occupied the major part of the total complexes. In the case of Pb-NACA, there were three complex forms with 1:1, 1:2 and 2:1 ratios. The Pb-NAC complex also had the 1:1 ratio form ass the major one, as in the Pb-NACA complex. After understanding the complex forms for Pb-NAC and Pb-NACA, a determination was made of the amount of lead chelated by the antioxidants, which required combination of data from ESI-MS and HPLC. The results of the HPLC experiment made it possible to estimate the percentage of antioxidants that had been reacted. Thus, the amount of lead reacted could be interpreted based on the relative abundance of the complex forms, and the ratios between the lead and NAC, NACA, and the antioxidants reacted.

The use of X-ray photoelectron spectroscopy (XPS) allowed a quick, but efficient estimate of the chelating abilities of different antioxidants. The percentage of Pb(II) could be determined by using XPS, in which case it was not possible to know the composition

of the multi-complexes and their relative percentages. The trend of chelating abilities obtained from the XPS experiment was consistent with the combination results from the ESI-MS and HPLC experiments, along with a comparison of their different point of zero charge values. NACA was determined to be better than NAC in chelating Pb(II) *in vitro*. The usual way to calculate the chelating ability of a compound is involved in knowing the structure of a complex, as well as its reacted percentage. As a result, a wide range of techniques, such ESI-MS, UV-vis spectrophotometer, HPLC and etc. are required to detect the exact chelating ability of a complex. By using X-ray photoelectron spectroscopy, it was more convenient and quick to assess the differentiated chelating abilities among antioxidants. However, the data obtained from the XPS experiment is not an absolute value, as it was not able to describe the exact chelating abilities of NAC and NACA, because it is a semi-quantification method. Using XPS, it is only possible to determine the percentage of lead reacted, but the amount of oxidation states of lead could not be determined. Thus, this technique could only estimate the trend of chelating abilities of the antioxidants. It is reasonable to assume that XPS is not a technique to be used for quantification, since it can only roughly determine a value.

Future research can be concentrated on an *in vivo* experiment that involves animal tests. An *In vitro* study comparing chelating abilities of NAC and NACA would be ideal for evaluation their relative efficacies in lead poisoning treatment, validating the predictive results in this study.

APPENDIX A

Retention time for Cysteamine, NAC and NACA in HPLC Experiments

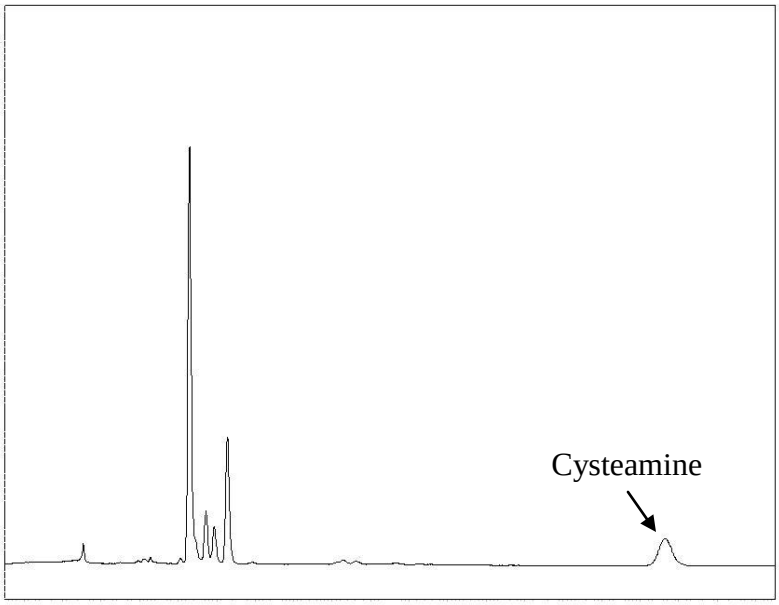

Retention time for Cysteamine is at 17.2 minutes

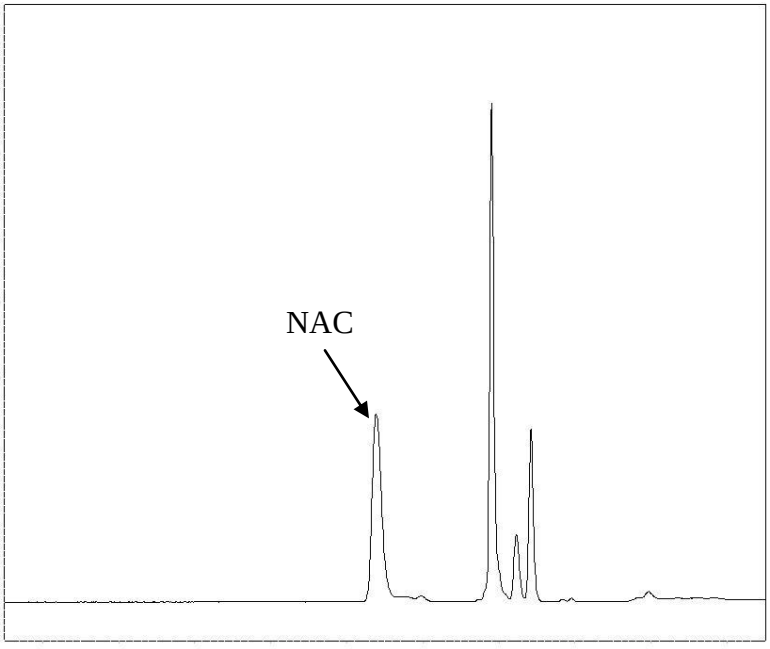

Retention time for NAC is at 4.8 minutes

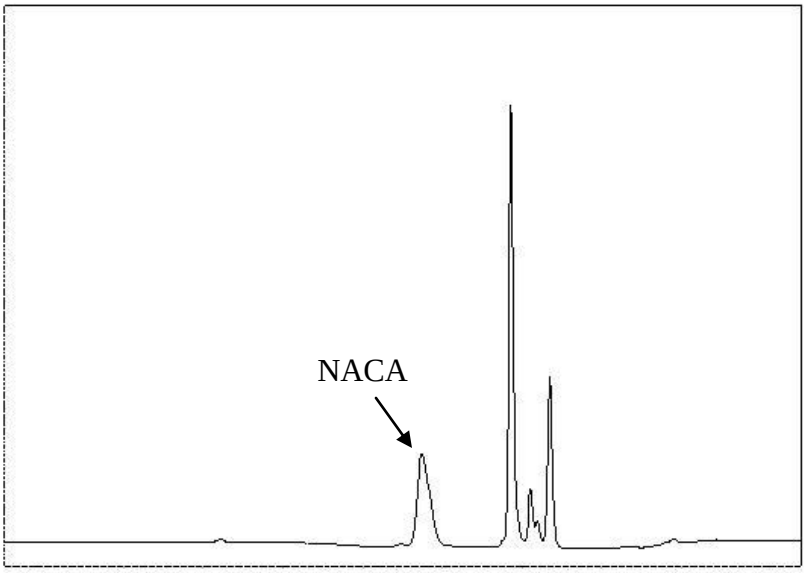

Retention time for NACA is at 5.2 minutes

REFERENCES

Aykin-Burns N. Franklin, E. A., Ercal N., Effects of N-Acetylcysteine on lead-exposed PC-12 cells, Arch. Environ. Contam. Toxicol. 2005, Vol 49, pp. 119-123.

Aykin-Burns N., Ercal N., Effects of selenocystine on lead-exposed Chinese hamster ovary (CHO) and PC-12 cells, Toxicol Appl Phamacol. 2006, Vol 214, pp. 136-143.

Barr T.L. Modern ESCA; CRC Press: Boca Raton, FL, 1994.

Bich C.,and Zenobi R., Mass spectrometry of large complexes, Curr Opin Structl Biol. 2009, Vol 19, pp. 632-639.

Blanusa M., Varnai V. M., Piasek M. and Kostial K., Chelators as antidotes of metal toxicity, Therapeutic and Experimental Aspects, Curr Med Chem. 2005, Vol 12, pp. 2771-2794.

Catton M. J. et al., Subclinical neuropathy in lead workers, Brit. Med. J. 1970, Vol 2, pp. 80.

CDC (Centers for Disease Control), Preventing lead poisoning in young children: a statement by the Centers for Disease Control. Atlanta, GA, CDC 1985, CDC report NO. 99-2230.

Fang XJ. and Fernando Q., Synthesis, structure, and properties of rac-2,3-mercaptosuccinic acid, a potentially useful chelating agent for toxic metals, Chem. Res. Toxicol. 1994, Vol 7, pp. 148-156.

Flora SJS, Bhattacharya R., Vijayaraghavan R., Combined therapeutic potential of Meso 2, 3 dimercaptosuccinic acid and calcium disodium edetate in experimental lead intoxication in rats, Fundam Appl Toxicol. 2005, Vol 25, pp. 233-240.

Flora S.J.S. et al., Heavy metal induced oxidative stress & its possible reversal by chelation therapy, Indian J. Med. Res. 2008, Vol 128, pp. 501-523.

Fonte R., Agosti A., Scafa F., Candura S.M., Anaemia and abdominal pain due to occupational lead poisoning, Haematologica 2007, Vol 92, pp. 13-14.

Gould E., Childhood Lead Poisoning: Conservative estimates of the social and economic benefits of lead hazard control, Environ Health Perspect. 2009, Vol 117, pp. 1162-1167.

Gupta V.K., Jain A.K. and Maheshwari G., Synthesis, characterization and Pb(II) ion selectivity of N, N' – bis(2 – hydroxyl – 1 - napthalene) – 2,6 – pyridiamine (BHNPD), Int. J. Electrochem. Sci. 2007, Vol 2, pp. 102-112.

Gurer H, Ercal N., Can antioxidants be beneficial in the treatment of lead poisoning? Free Radic Biol Med. 2000, Vol 29, pp. 927-945.

Hagstrom S., Nordling C., and Siegbahn K., Z. physic. 1964, Vol 178: pp. 439.

Handley M. A., Sanford CHE., Diaz E., Gonzalez-Mendez E., Drace K., Wilson R., Villalobos M., and Croughan M., Globalization, binational, communities, and imported food risks: results of an outbreak investigation of lead poisoning in Montery county, California, Am J Public Health. 2007 Vol 97: pp. 900-906.

Hollander J.M. and Jolly W.L., X-ray photoelectron spectroscopy, Acc. Chem. Res. 1970, Vol 3: pp. 193-200.

Horowitz B. Z., and Mirkin D. B., Lead poisoning and chelation in a mother-neonate pair, Clin Toxicol. 2001, Vol 39, pp. 727–731.

Iribarne JV, Thomson BA., On the evaporation of charged ions from small droplets, J Chem Phy. 1976, Vol 64, pp. 2287– 2294.

Karri S. K., Saper R. B., and Kales S. N., Lead encephalopathy due to traditional medicines, Curr Durg Saf., 2008, Vol 3: pp. 54-59.

Kebarle P., Peschke M., On the mechanisms by which the charged droplets produced by electrospray lead to gas phase ions, Anal. Chim. Acta. 1999, Vol 20070, pp. 1–25.

Kidd P., Glutathione: Systemic protectant against oxidative and free radical damage, Altern Med Rev. 1997, Vol 2: pp. 155-176.

Landrigan P. J. and Todd A. C., Lead poisoning, West J Med. 1994, Vol 161: pp. 153-159.

MacCarthy P. and Mark H. B., Jr., An evaluation of Job's method of continuous variations as applied to soil organic matter-metal ion interactions, Soil Sci Soc Am J. 1976, Vol 40, pp. 267-276.

Mathee A., Röllin H., Levin J., and Naik I., Lead in paint : three decades later and still a hazard for African children, Environ. Health Perspect. 2007, Vol 115, pp. 321-322.

Mitchell R. A., Drake J. E., Wittlin L. A., and Rejent T. A., Erythrocyte porphobilinogen synthase (delta-aminolaevulinate dehydratase) activity: a reliable and quantitative indicator of lead exposure in humans, Clin. Chem. 1977, Vol 23: pp. 105-111.

Park J. and Regalbuto J. R., J. Colloid Interface Sci. 1995, 175, pp. 239.

Patrick ND., Lead toxicity, a review of the literature. Part I: exposure, evaluation, and treatment, Altern Med Rev. 2006, Vol 11, pp. 2-22.

Patrick ND., Lead toxicity part II: the role of free radical damage and the use of antioxidants in the pathology and treatment of lead toxicity, Altern Med Rev. 2006, Vol 11, pp. 114-127.

Penugonda S., Mare S., Lutz P., Banks W. A., Ercal N., Potentiation of lead-induced cell death in PC12 cells by glutamate: Protection by *N*- acetylcysteine amide (NACA), a novel thiol antioxidant, Toxicol. Appl Pharmacol. 2006, Vol 216, pp. 197-205.

Porru S. and Alessio L., The use of chelating agents in occupational lead poisoning, Occp. Med., 1996, Vol 46, pp. 41-48.

Purser D. A., Berrill K. R., and Majeed S. K., Effects of lead exposure on peripheral nerve in the cynomolgus monkey, Br J Ind Med. 1983, Vol 40, pp. 402-412.

Ribarov SR., Benov LC., Relationship between the hemolytic action of heavy metals and lipid peroxidation, Biochim Biophys Acta, 1981, Vol 640: pp. 721-726.

Ryter S. W. and Tyrrell R. M., The heme synthesis and degradation pathways: role in oxidant sensitivity, heme oxygenase has both pro- and antioxidant properties, Free Radic Biol Med. 2000, Vol 28, pp. 289–309.

Sandhir R,. Julka D., Gill KD., Lipoperoxidative damage on lead exposure in rat brain and its implications on membrane bound enzymes, Pharmacol Toxicol, 1994, Vol 74: pp. 66-71.

Shobha N., Taly A. B., Sinha S., and Venkatesh T., Radial neuropathy due to occupational lead exposure: Phenotypic and electrophysiological characteristics of five patients, Ann Indian Acad Neurol. 2009, Vol 12, pp. 111-115.

Siegbahn K., Nordling C., Fahlman A., Nordberg R., Hamrin K., Hedman J., Johansson G., Bergmark T., Karlsson S.-E., Lindgren I., and Lindberg B., ESCA; Atomic, Molecular and Solid State Structure by Means of Electron Spectroscopy, Almqvist and Wiksells, Uppsala 1967, pp. 21.

Stangle DE., Smith DR., Beaudin SA., Strawderman MS., Levitsky DA., Strupp BJ., Succimer chelation improves learning, attention, and arousal regulation in lead-exposed rats but produces lasting cognitive impairment in the absence of lead exposure, Environ Health Perspect. 2007, Vol 115, pp. 201-209.

Taflin DC., Ward TL., Davis EJ., Electrified droplet fission and the Rayleigh limit, Langmuir 1989, Vol 5, pp.376–384.

Tzu D., Tan L., Lin JL., Yen TH., Chen KH., and Huang YL., Long-term outcome of repeated lead chelation therapy in progressive non-diabetic chronic kidney diseases, Nephrol Dial Transplant. 2007, Vol 22, pp. 2924–2931.

Wu W., GoldsteinG., Adams C., Matthews R. H. and Ercal N., Separation and quantification of N-acetyl-L-cysteine and N-acetyl-cysteine-amide by HPLC with fluorescence detection, Biomed Chromatogr. 2006, Vol 20, pp. 415-422.

Young V. Y. and Williams K. R., X-ray photoelectron spectroscopy of aluminum oxalate tetrahydrate, J. Electron Spectrosc. Relat. Phenom. 1999, Vol 104, pp. 221-232.

Youssef N. F. and Taha E.A., Development and validation of spectrophotometric, TLC and HPLC methods for the determination of lamotriqine in presence of its impurity, Chem. Pharm. Bull., 2007, Vol 55: pp. 541-545.

Zhang J., Wang XF., Lu ZB., Liu NQ., and Zhao VL., The effects of *MESO*-2,3-Dimercaptosuccinic acid and oligomeric procyanidins on acute lead neurotoxicity in rat hippocampus, Free Rad Biol Med. 2004, Vol 37, pp. 1037-1050.

Zhao Y., Wang L., Shen HB, Wang ZX., Wei QY., Chen F., Association between delta-aminolevulinic acid dehydratase (ALAD) polymorphism and blood lead levels: a meta-regression analysis, J Toxicol Environ Health A. 2007, Vol 70: pp. 1984-1994.

VITA

Weiqing Chen was born on January 9, 1985, in Jiaxing, Zhejiang Province, China. After receiving her primary and secondary education in Jiaxing, she studied at East China Normal University in Shanghai, China, and received a bachelor degree in Biological Sciences in June 2007. Since the summer of 2008, she has been enrolled in the graduate school majoring in Chemistry at Missouri University of Science and Technology, Rolla, MO, U.S.A. She graduated from Missouri S&T with a Master's Degree in May 2010.